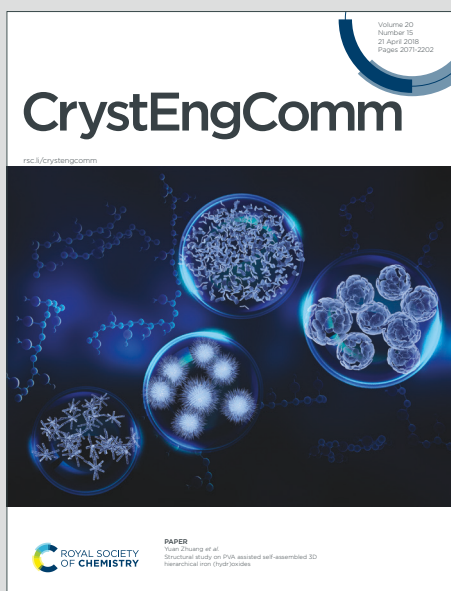


CrystEngComm

Accepted Manuscript

This article can be cited before page numbers have been issued, to do this please use: S. Sofronova, E. Moshkina, A. Chernyshev, A. D. Vasil'ev, N. Maximov, A.S. Aleksandrovsky, T. Andryushchenko and A. Shabanov, *CrystEngComm*, 2024, DOI: 10.1039/D4CE00091A.



This is an Accepted Manuscript, which has been through the Royal Society of Chemistry peer review process and has been accepted for publication.

Accepted Manuscripts are published online shortly after acceptance, before technical editing, formatting and proof reading. Using this free service, authors can make their results available to the community, in citable form, before we publish the edited article. We will replace this Accepted Manuscript with the edited and formatted Advance Article as soon as it is available.

You can find more information about Accepted Manuscripts in the [Information for Authors](#).

Please note that technical editing may introduce minor changes to the text and/or graphics, which may alter content. The journal's standard [Terms & Conditions](#) and the [Ethical guidelines](#) still apply. In no event shall the Royal Society of Chemistry be held responsible for any errors or omissions in this Accepted Manuscript or any consequences arising from the use of any information it contains.

Crystal growth and cation order of $\text{Ni}_{3-x}\text{Co}_x\text{B}_2\text{O}_6$ oxyborates

Svetlana Sofronova^a, Evgeniya Moshkina^a, Artem Chernyshev^a, Aleksandr Vasilev^a, Nikolai G. Maximov^b, Aleksandr Aleksandrovsky^a, Tatyana Andryushchenko^a, Aleksandr Shabanov^a

View Article Online

DOI: 10.1039/C4CY01596A

^a*Kirensky Institute of Physics of the Federal Research Center "Krasnoyarsk Science Center of the Siberian Branch of the Russian Academy of Sciences", 660036 Krasnoyarsk, Russia*

^b*Institute of Chemistry and Chemical Technology SB RAS, Federal Research Center*

"Krasnoyarsk Science Center SB RAS", Russia

Abstract

A series of single crystals of $\text{Ni}_{3-x}\text{Co}_x\text{B}_2\text{O}_6$ compounds with the kotoite structure and with different concentrations of transition metal ions ($x = 0; 0.19; 0.6; 0.93$ and 2) were obtained. The lattice parameters and atomic coordinates were determined using X-ray diffraction. The theoretical calculations using the WIEN2k package predict that nickel ions tend to occupy the 4f crystallographic position, while cobalt ions tend to occupy the 2a crystallographic position. The study of the diffuse scattering spectra and comparison of the Racah parameters for the compounds $\text{Ni}_3\text{B}_2\text{O}_6$ and $\text{Co}_2\text{NiB}_2\text{O}_6$ provides experimental evidence that nickel ions occupy crystallographic position 4f.

Introduction

Recently, oxyborates $\text{M}_3\text{B}_2\text{O}_6$ (where M are Co, Ni, Mn) have attracted great interest due to their potential use as anode materials for lithium-ion and sodium-ion battery cells [1-7]. There have been a number of studies which show oxyborate $\text{Ni}_3\text{B}_2\text{O}_6$ to be a highly promising anode material for sodium-ion batteries [1, 2, 3, 6, 7]. These studies were carried out on ceramic samples. The $\text{Ni}_3\text{B}_2\text{O}_6$ electrode is known to have a reversible capacity of $428,9 \text{ mAh g}^{-1}$ at 200 mA g^{-1} . Even at a very high current density of 2000 mA g^{-1} the specific capacity of $\text{Ni}_3\text{B}_2\text{O}_6$ remains to be equal to $304,4 \text{ mAh g}^{-1}$ [1]. Although $\text{Ni}_{3-x}\text{Co}_x\text{B}_2\text{O}_6$ oxyborates with the kotoite structure have long been known, and the structural, optical and magnetic properties of $\text{Ni}_3\text{B}_2\text{O}_6$ and $\text{Co}_3\text{B}_2\text{O}_6$ have widely been studied, there is little information on the solid solutions of $\text{Ni}_{3-x}\text{Co}_x\text{B}_2\text{O}_6$. However, the study of the $\text{Ni}_{3-x}\text{Co}_x\text{B}_2\text{O}_6$ solid solutions can provide a key to the solution of some fundamental problems. In particular, both isostructural kotoites $\text{Ni}_3\text{B}_2\text{O}_6$ and $\text{Co}_3\text{B}_2\text{O}_6$ are antiferromagnetic, but the easy axis of magnetization is different, with one being directed along the c axis in $\text{Ni}_3\text{B}_2\text{O}_6$, and the other along the b axis in $\text{Co}_3\text{B}_2\text{O}_6$ [8]. The investigation of the lattice dynamics of $\text{Ni}_3\text{B}_2\text{O}_6$ shows several new phonon modes to appear at the antiferromagnetic ordering temperature [9], while in $\text{Co}_3\text{B}_2\text{O}_6$ such effects are not observed

[10]. The studies in [11,12] report on the synthesis of the compounds $\text{Co}_2\text{NiB}_2\text{O}_6$ and $\text{CoNi}_2\text{B}_2\text{O}_6$, and present the information on the crystal structure and crystal lattice constants. However, the physical properties of these compounds have not thoroughly been studied yet.

The existence of cobalt and nickel kotoites, as well as, the information on the synthesis of the compounds $\text{Co}_2\text{NiB}_2\text{O}_6$ and $\text{CoNi}_2\text{B}_2\text{O}_6$ make it possible to form a great number of $\text{Ni}_{3-x}\text{Co}_x\text{B}_2\text{O}_6$ solid solutions with the kotoite structure with different concentrations of nickel and cobalt ions. Obtaining $\text{Ni}_{3-x}\text{Co}_x\text{B}_2\text{O}_6$ solid solutions is difficult due to the fact that cobalt ions can change their valence state and they can be crystallized in the Co_3BO_5 ludwigite phase. Thus, in order to obtain crystals of the kotoite phase $\text{Ni}_{3-x}\text{Co}_x\text{B}_2\text{O}_6$ from a flux, it is necessary to control the valence of cobalt cations as well as to investigate the stability of this phase upon changing the Co/Ni ratio in the flux. In the present study, we have made an attempt to obtain a number of $\text{Ni}_{3-x}\text{Co}_x\text{B}_2\text{O}_6$ compounds with the kotoite structure with different concentrations of transition metal ions, to study the crystal structure of the obtained compounds by theoretical and experimental methods, as well as to reveal the distribution of transition metal ions over the crystallographic positions.

Crystal growth.

The present study is devoted to crystallization of Ni-Co borates in the flux system based on $\text{Bi}_2\text{Mo}_3\text{O}_{12}\text{-B}_2\text{O}_3$, diluted with Na_2CO_3 carbonate, with the aim of obtaining $\text{Ni}_{3-x}\text{Co}_x\text{B}_2\text{O}_6$ solid solutions with the kotoite structure. The flux system under study had the form:

$$\begin{aligned} & (100 - n)\% \text{ mass. } (\text{Bi}_2\text{Mo}_3\text{O}_{12} + 0.8\text{Na}_2\text{O} + p\text{B}_2\text{O}_3 + q\text{Co}_2\text{O}_3) + \\ & n\% \text{ mass. } ((2 - x)\text{CoO} + x\text{NiO} + 0.5\text{Co}_2\text{O}_3 + 0.5\text{B}_2\text{O}_3) \end{aligned} \quad (1)$$

The samples were grown in air at atmospheric pressure using a resistant furnace equipped with silicon carbide heaters. The concentration of the crystal-forming oxides n , molar coefficients p and q , starting temperature T_{start} for obtaining single crystal samples and the corresponding nickel content x are given in Table 1. The fluxes were prepared by successive melting of the powder mixture of system (1) in a platinum crucible ($V = 100 \text{ cm}^3$) at temperature $T = 1100^\circ\text{C}$ in the following order: first, the mixture $\text{B}_2\text{O}_3 - \text{Bi}_2\text{O}_3 - \text{MoO}_3$ was molten, then Na_2CO_3 was introduced in portions (in writing the first system, use was made of Na_2O due to the decomposition of carbonate into oxide and carbon dioxide at high temperatures), and further, Co_2O_3 and Ni_2O_3 were successively added in portions. The trioxides Ni_2O_3 and Co_2O_3 were used instead of the dioxides NiO and CoO , respectively, for the flux preparation due to the temperatures of the decomposition of trioxides to (II,III) oxides and, finally, to dioxides being low (the highest one is $T = 905\text{-}925^\circ\text{C}$ for the reaction $2\text{Co}_3\text{O}_4 \rightarrow 6\text{CoO} + \text{O}_2\uparrow$). Thus, at the preparation stage the flux system should contain only bivalent cations of Co and Ni. Then, due to the presence of the MoO_3

and Na₂O solvent components the valence state of Co cations can be stabilized following the mechanisms discussed in [13, 14].

View Article Online
DOI: 10.1039/D4CE00091A

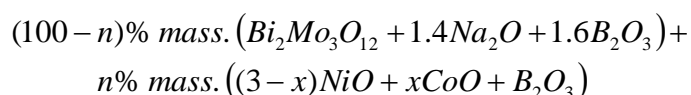
After the decomposition of all the components, the fluxes were kept at $T = 1100^{\circ}\text{C}$ for three hours. After the stage of homogenization, a high temperature crystallizing phase (HTCP) corresponding to each composition of system (1) and the parameters of the flux were determined. The detailed description of the procedure is given in [15]. Then, there followed the crystal growth: after another homogenization of the flux at $T = 1100^{\circ}\text{C}$, the temperature in the furnace was first decreased at a high rate, $100^{\circ}\text{C}/\text{h}$, and then, slowly at a rate of $4^{\circ}\text{C}/\text{day}$. After 24 hours, the flux was removed from the crucible, the obtained crystals were taken from the crucible and the remainder of the flux was also removed by etching in a 20% solution of nitric acid.

Table 1. The parameters of flux system (1).

Stage	x	p	q	$n, \%$	$T_{\text{start}}, ^{\circ}\text{C}$	Crystal structure
1	0.25	0.6	0.5	12		ludwigite
2	0.44	0.56	0.45	13.64	950	ludwigite
3	0.58	0.53	0.42	15		kotoite
4	0.7	0.51	0.29	12.9	900	ludwigite

The nickel content x in the flux changed from 0 to 0.7. The addition of nickel oxide into flux system (1) followed four stages, with the visual observation of the substance being crystallized; after the second and fourth additions, two successive samples were taken for each of the additions. With the nickel content $x = 0.25$ and 0.44 , crystallization of black elongated crystals was observed, corresponding to the phase of ludwigite $\text{Co}^{3+}\text{Ni}^{2+}_{2-x}\text{Co}^{2+}_x\text{BO}_5$. In the case of adding large amounts of nickel oxide (at 0.58 up to 0.7), it was possible to see joint crystallization of black elongated crystals corresponding to the ludwigite phase and that of green isometric crystals corresponding to the kotoite phase. Thus, despite the chosen small concentrations of nickel, the appearance of joint crystallization along with the ludwigite phase indicates the proximity of the phase boundaries for the obtained compositions and gives evidence for the existence of the Co-Ni kotoite phase in the narrow concentration range.

Thus, due to the proximity of the kotoite/ludwigite phase boundaries, flux system (1) needs to be finalized to obtain Ni-Co kotoites. The desired borates $\text{Ni}_{3-x}\text{Co}_x\text{B}_2\text{O}_6$ contained only bivalent transition metal cations unlike $\text{Co}^{3+}\text{Ni}^{2+}_{2-x}\text{Co}^{2+}_x\text{BO}_5$ ludwigites. Therefore, it was necessary to minimize the quantity of trivalent cobalt cations in the flux. A new flux system for growing $\text{Ni}_{3-x}\text{Co}_x\text{B}_2\text{O}_6$ was the following:



View Article Online
DOI: 10.1039/D4CE00091A

The concentration of the crystal-forming oxides n was varied in the range of 5-10%, the corresponding cobalt composition x was changed in the range of 0-1.33. In contrast to system (1), system (2) included the following changes: Co_2O_3 was removed from the solvent, and the portions of Na_2O and B_2O_3 were increased. However, the ratio Na_2O/B_2O_3 was decreased significantly, reducing the possibility of the presence of sodium oxide which is not coupled by chemical bonds in borax $Na_2B_4O_7$. Due to the possibility of the formation of intermediate chemical bonds such as in delafossite $NaCo^{3+}O_2$, the amount of Na_2O oxide in the flux in the “pure” form can significantly influence the probability of the presence of Co^{3+} cations, including the crystallizing phase.

The high temperature crystallizing phase of system (2) was the phase of $Ni_{3-x}Co_xB_2O_6$ borates with the kotoite structure in a wide temperature range (at least 40 °C). The saturation temperature of the flux varied within 840-900°C, depending on the concentration x . Four out of the obtained single crystals $Ni_{3-x}Co_xB_2O_6$ with the cobalt concentration $x = 0, 0.5, 1.125$ and 1.33 were formed from flux system (2). Thus, five compositions of $Ni_{3-x}Co_xB_2O_6$ were obtained. The images of these single crystals are presented in Fig. 1.

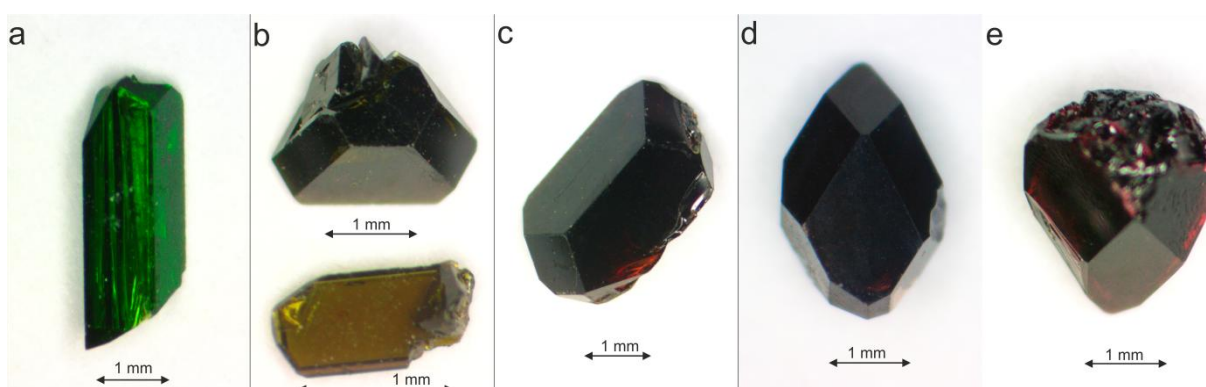


Figure. 1. The images of $Ni_{3-x}Co_xB_2O_6$ single crystals with the kotoite structure: $x = 0$ (a), $x = 0.5$ (b), $x = 1.125$ (c), $x = 1.33$ (d), $x = 2.3$ (e) (the cobalt concentrations are given with regard to the flux composition).

Structure and composition of the compounds

The obtained single crystals were studied with a table top scanning electron microscope Hitachi TM-4000Plus at an accelerating voltage of 20 kV. The elemental mapping was performed using an X-ray detector Bruker XFlash 630Hc. The spectra were analyzed with the software Quantax70. All the samples were homogenous in the composition. To test the homogeneity, the spectra from different areas of the crystals were compared for all the groups of samples.

The concentration of cobalt ions of the four samples refined by scanning electron microscopy along with their concentration in the flux are presented in Table 2. As is seen in the table, there is a qualitative agreement between the composition in the flux and the real nickel and cobalt content in the compounds, however, the real nickel content exceeds the one in the flux, which emphasizes the difference in the distribution coefficients of nickel and cobalt oxides in the fluxes used: the lower solubility of nickel oxide results in larger content of this element in the crystal [15].

In addition, we used the X-ray fluorescence analysis to estimate the concentration of cobalt and nickel ions in the crystals. Characteristic X-ray spectra were obtained using a local X-ray fluorescence spectrometer MC50M (Amtertek, Russia) and additional PXRF software. The accelerating voltage of the X-ray source was 30 kV with the current of 20 μ A, and exposure time of 100 s. Calculation of the element concentrations was carried out based on the Sherman fundamental parameter method [16] with the correction of matrix effects based on the values of the integral intensities of the main lines (100% normalization). The obtained results are also presented in Table 2. As one can see from the table, both methods give similar concentrations of cobalt ions in the compounds. The crystal structure of the single crystal samples was studied by the method of x-ray diffraction at room temperature using a diffractometer SMART APEXII (Mo $K\alpha$, $\lambda=0,7106$ Å). The study of the crystal structure of all the $Ni_{3-x}Co_xB_2O_6$ compounds showed the space symmetry group to be $Pnmm(58)$. The lattice constants and atomic coordinates are presented in Table 3.

Table 2. The comparison between the real composition of the obtained samples and the composition in the flux for each sample.

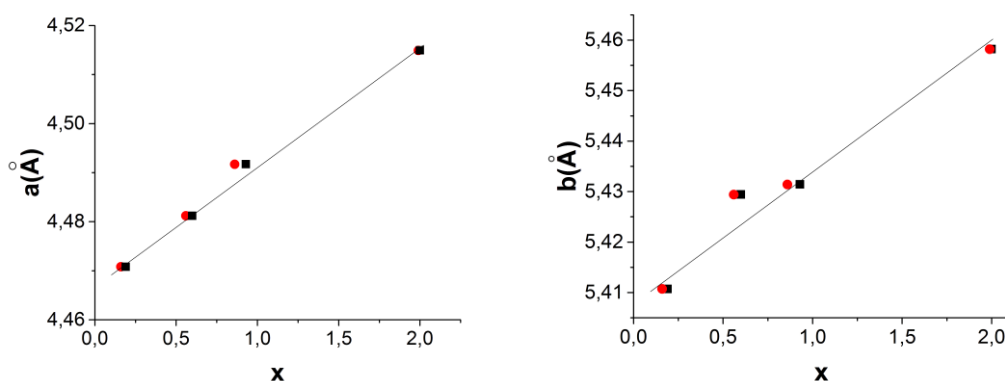
Sample no.	Co concentration in the flux	Co concentration in the crystal	
		scanning electron microscopy	X-ray fluorescence analysis
S1	0.5	0.19	0.16
S2	1.125	0.60	0.56
S3	1.33	0.93	0.86
S4	2.3	2	1.99

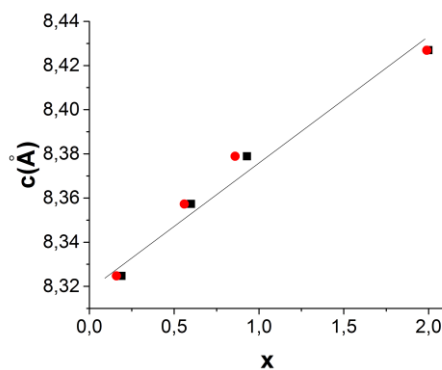
Table 3. The lattice constants and atomic coordinates of the compound $\text{Co}_{3-x}\text{Ni}_x\text{B}_2\text{O}_6$ with the kotoite structure.

View Article Online
DOI: 10.1039/D4CE00091A

Compounds		S1	S2	S3	S4
Lattice constants					
a (Å)		4.4708(2)	4.4813(5)	4.4917(6)	4.5149(2)
b (Å)		5.4107(3)	5.4294(5)	5.4314(8)	5.4582(3)
c (Å)		8.3247(4)	8.3573(8)	8.3789(12)	8.4269(5)
Atom	Position	Atomic coordinates (x/a; y/b; z/c)			
Co/Ni	4f	0; 1/2; 0.81571(5)	0; 1/2; 0.81539(5)	0; 1/2; 0.81522(4)	0; 1/2; 0.81438(4)
Co/Ni	2a	1/2; 1/2; 1/2	1/2; 1/2; 1/2	1/2; 1/2; 1/2	1/2; 1/2; 1/2
O ₁	8h	0.2019(3); 0.2982(2); 0.63995(17)	0.2020(3); 0.2982(2); 0.63992(16)	0.2013(2); 0.29748(19); 0.63961(13)	0.1996(3); 0.2956(2); 0.63897(14)
O ₂	4g	0.7466(4); 0.1755(4); 1/2	0.7478(4); 0.1766(4); 1/2	0.7475(3); 0.1771(3); 1/2	0.7483(4); 0.1788(3); 1/2
B	4g	0.0427(8); 0.2457(6); 1/2	0.0422(7); 0.2457(6); 1/2	0.0432(5); 0.2457(4); 1/2	0.0439(6); 0.2457(5); 1/2

Figure 2 presents the concentration dependences of the lattice parameters, where x is the concentration of cobalt ions. The black squares denote the experimental data obtained by scanning electron microscopy, while the red circles denote the results obtained by the X-ray fluorescence analysis. The concentration dependences are in good agreement with the Vegard law for solid solutions.





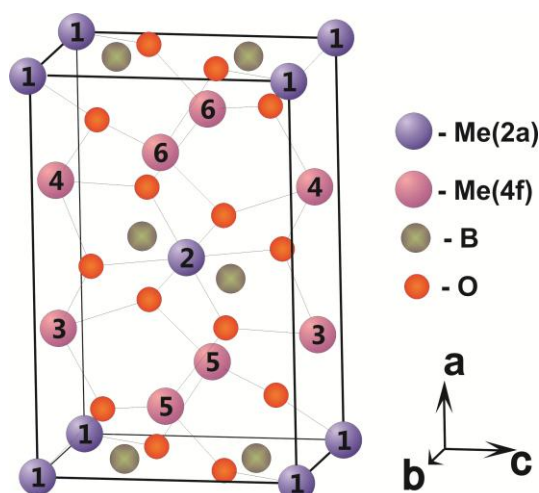
View Article Online
DOI: 10.1039/D4CE00091A

Fig. 2. The dependences of the lattice parameters a , b , c on the concentration x of cobalt ions.

Cationic ordering of transition metal ions. First-principles calculation.

It is impossible to distinguish between nickel and cobalt ions using X-ray diffraction as they have the same electronic configuration. In order to specify the distribution of transition metal ions over crystallographic positions, we calculated the energies of various cation-ordered configurations based on the first energy principles. Similar calculations were used to search for the most stable ordering of Mg/Fe in site A and Si/Al in site B in the FA50 bridgmanite [17] or to study the impacts of cation ordering on changes in the electronic structure in double perovskites [18] and to study the structural principles and energies of A-site ordered AA'B₂O₆ double perovskites [19]. The calculation of the energy of various configurations for the Ni₂Co(BO₃)₂ and Co₂NiB₂O₆ compounds was performed by the FP-LAPW+lo method [20, 21] using the Wien2K software package. The exchange-correlation energy was calculated using LSDA [22] and GGA-PBE [23] with additional Hubbard correlation coefficients describing the local electron-electron repulsion associated with 3d bands of Ni, Co (LSDA U and GGA-PBE+U) [24, 25]. The electron configuration of the atoms used in our calculations was: [Ar] 3d⁸ 4s² for Ni, [Ar] 3d⁷ 4s² for Co, [He] 2s² 2p¹ for B and [He] 2s² 2p⁴ for O. All the calculations were made using the experimental lattice constants and atomic coordinates.

The unit cell of kotoite includes 6 transition metal atoms. In Figure 3 these are indicated by the blue circles, with the atoms numbered 1 and 2 corresponding to crystallographic position 2a, and those with numbers 3-6 corresponding to crystallographic position 4f. The Co₂NiB₂O₆ compound has two nickel ions and four cobalt ions in the unit cell, while the Ni₂Co(BO₃)₂ compound has four nickel ions and two cobalt ions in the unit cell. In the solid solution Ni_{2.5}Co_{0.5}(BO₃)₂ there is only one cobalt ion in the unit cell. We distributed nickel and cobalt ions in different ways over positions 1-6 (Fig. 3) and calculated the total energy of the crystal.



View Article Online
DOI: 10.1039/D4CE00091A

Fig. 3. The crystal structure of kotoite. The positions of transition metal ions are denoted by the blue circles and numbered as 1-6. Positions 1 and 2 correspond to crystallographic position 2a while positions 3, 4, 5 and 6 correspond to crystallographic position 4f.

Tables 4, 5 and 6 show the calculation results for several different cation-ordered configurations for $\text{Co}_2\text{NiB}_2\text{O}_6$, $\text{Ni}_2\text{Co}(\text{BO}_3)_2$ and $\text{Ni}_{2.5}\text{Co}_{0.5}(\text{BO}_3)_2$. In $\text{Co}_2\text{NiB}_2\text{O}_6$ the cation-ordered configuration (№ 6) with the minimum energy is shown in Figure 4a. As is seen from the Figure, nickel ions tend to occupy the 4f position, and in addition, in such a way so as to be as far apart from each other as possible. In $\text{Ni}_2\text{Co}(\text{BO}_3)_2$ the cation-ordered configuration (№ 1) with the minimum energy is shown in Figure 3b. There, cobalt ions tend to occupy the 2a position. In $\text{Ni}_{2.5}\text{Co}_{0.5}(\text{BO}_3)_2$ the single cobalt ions also tend to occupy the 2a position. Irrespectively of the site (1 or 2) in the 2a position which the single cobalt ions tend to occupy, the full energies are equal. The same applies to the position 4f

Table 4. The calculated energy values of the cation-ordered configurations in $\text{Co}_2\text{NiB}_2\text{O}_6$ with different distributions of Ni and Co ions over positions 1-6.

№	1	2	3	4	5	6	E(a.u.)
	2a	2a	4f	4f	4f	4f	
1	Co	Co	Ni	Ni	Co	Co	-19236.3642
2	Ni	Ni	Co	Co	Co	Co	-19236.3402
3	Ni	Co	Ni	Co	Co	Co	-19236.3529
4	Ni	Co	Co	Co	Ni	Co	-19236.3518
5	Co	Co	Ni	Co	Ni	Co	-19236.3672
6	Co	Co	Co	Ni	Ni	Co	-19236.3688
7	Co	Co	Ni	Co	Co	Ni	-19236.3688

Table 5. The calculated total energies of various cation-ordered configurations in $\text{Ni}_2\text{Co}(\text{BO}_3)_2$.

View Article Online
DOI: 10.1039/D4CE00091A

№	1	2	3	4	5	6	E(a.u.)
	2a	2a	4f	4f	4f	4f	
1	Co	Co	Ni	Ni	Ni	Ni	-19745.8722
2	Ni	Co	Co	Ni	Ni	Ni	-19745.8269
3	Co	Ni	Co	Ni	Ni	Ni	-19745.8264
4	Ni	Ni	Co	Co	Ni	Ni	-19745.7855
5	Ni	Ni	Ni	Co	Ni	Co	-19745.7836
6	Ni	Ni	Co	Ni	Ni	Co	-19745.7828

Table 6. The calculated total energies of various cation-ordered configurations in $\text{Ni}_{2,5}\text{Co}_{0,5}(\text{BO}_3)_2$.

№	1	2	3	4	5	6	E(a.u.)
	2a	2a	4f	4f	4f	4f	
1	Co	Ni	Ni	Ni	Ni	Ni	-20000.4249
2	Ni	Co	Ni	Ni	Ni	Ni	-20000.4249
3	Ni	Ni	Co	Ni	Ni	Ni	-20000.4130
4	Ni	Ni	Ni	Ni	Ni	Co	-20000.4130

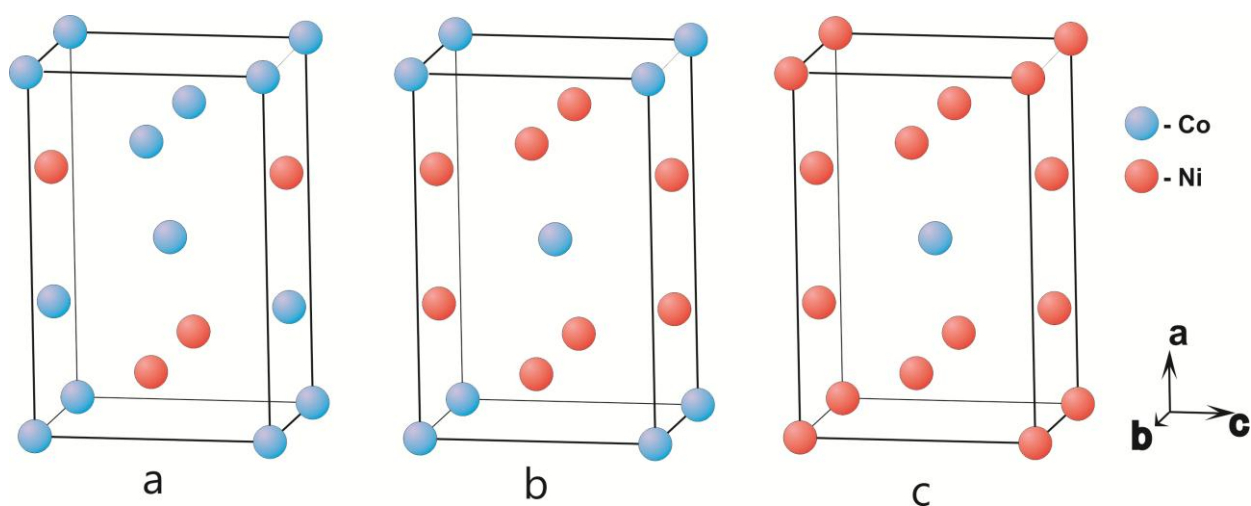


Fig. 4. The most advantageous cation-ordered configuration in $\text{Co}_2\text{NiB}_2\text{O}_6$ (a), $\text{Ni}_2\text{Co}(\text{BO}_3)_2$ (b) and $\text{Ni}_{2,5}\text{Co}_{0,5}(\text{BO}_3)_2$ (c).

Cationic ordering of transition metal ions. Spectroscopy of electronic excitations in cobalt and nickel kotoites.

In order to experimentally establish how nickel and cobalt ions are distributed over crystallographic positions, it is necessary to carry out an investigation by neutron diffraction; however, this method is not such an accessible tool as the X-ray diffraction method. There are a number of other studies that may indirectly indicate the occupation of one or another position by ions of the same type. The spectral properties of $\text{Co}_3\text{B}_2\text{O}_6$ in the area of electronic excitations were studied in [21], and the spectra of an arbitrarily oriented $\text{Ni}_3\text{B}_2\text{O}_6$ single crystal in a wide temperature range up to 5 K were investigated in detail and analyzed at a high level in [22]. In the study by Molchanova it was shown that the absorption spectra of Ni^{2+} ions were split, since the nickel ion occupied two crystallographic positions. For each position (2a and 4f), the Racah parameters were determined, and the difference in the coefficients turned out to be rather significant. In this work, we also examined diffuse scattering spectra for $\text{Co}_2\text{NiB}_2\text{O}_6$ and determined the Racah parameters in order to carry out a comparative analysis with kotoites $\text{Ni}_3\text{B}_2\text{O}_6$, $\text{Co}_3\text{B}_2\text{O}_6$.

Diffuse scattering spectra of $\text{Ni}_3\text{B}_2\text{O}_6$, $\text{Co}_3\text{B}_2\text{O}_6$ and $\text{Co}_2\text{NiB}_2\text{O}_6$ were obtained using pressed microcrystalline powders on a Shimadzu UV-3600 spectrometer with an integrated sphere. The Kubelka-Munk functions of $\text{Ni}_3\text{B}_2\text{O}_6$, $\text{Co}_3\text{B}_2\text{O}_6$, and $\text{Co}_2\text{NiB}_2\text{O}_6$ obtained from the diffuse reflectance measurements are presented in Fig. 5. In the spectrum of $\text{Co}_3\text{B}_2\text{O}_6$ the spin-allowed transitions from the ground state $^4\text{T}_1(^4\text{F})$ of the Co^{2+} ion to the $^3\text{T}_2(^3\text{F})$ (1350 nm), $^4\text{A}_2(^4\text{F})$ (690 nm) and $^4\text{T}_1(^4\text{P})$ (535 nm) excited states are well-pronounced. Splitting of the $^4\text{T}_1(^4\text{F}) \rightarrow ^4\text{T}_2(^4\text{F})$ band can be ascribed mainly to the existence of two non-equivalent Co sites in the crystal structure of kotoite, and, to a lower extent, to the distortion of the CoO_6 octahedra. In the spectrum of $\text{Ni}_3\text{B}_2\text{O}_6$ the spin-allowed transitions from the ground state $^3\text{A}_2(^3\text{F})$ of the Ni^{2+} ion to the $^3\text{T}_2(^3\text{F})$ (1370 and 1190 nm), $^3\text{T}_1(^3\text{F})$ (756 nm) and $^3\text{T}_1(^3\text{P})$ (423 nm) excited states can easily be observed. The $^3\text{A}_2(^3\text{F}) \rightarrow ^3\text{T}_1(^3\text{P})$ band of Ni^{2+} is split similarly to the visible band of Co^{2+} ; however, one of the split components is obviously dominant in the case of Ni^{2+} . Strong splitting is observed in the case of the infrared Ni^{2+} band at the $^3\text{A}_2(^3\text{F}) \rightarrow ^3\text{T}_2(^3\text{F})$ transition. An additional narrow peak on the $^3\text{A}_2(^3\text{F}) \rightarrow ^3\text{T}_1(^3\text{F})$ band, on the contrary, can be ascribed to the contribution from spin-forbidden $^3\text{A}_2(^3\text{F}) \rightarrow ^1\text{E}(^1\text{D})$. The spectrum of $\text{Co}_2\text{NiB}_2\text{O}_6$ is merely a mixture of individual spectra of the cobalt and nickel kotoites with no signs of the mutual influence of the Co and Ni sublattices.

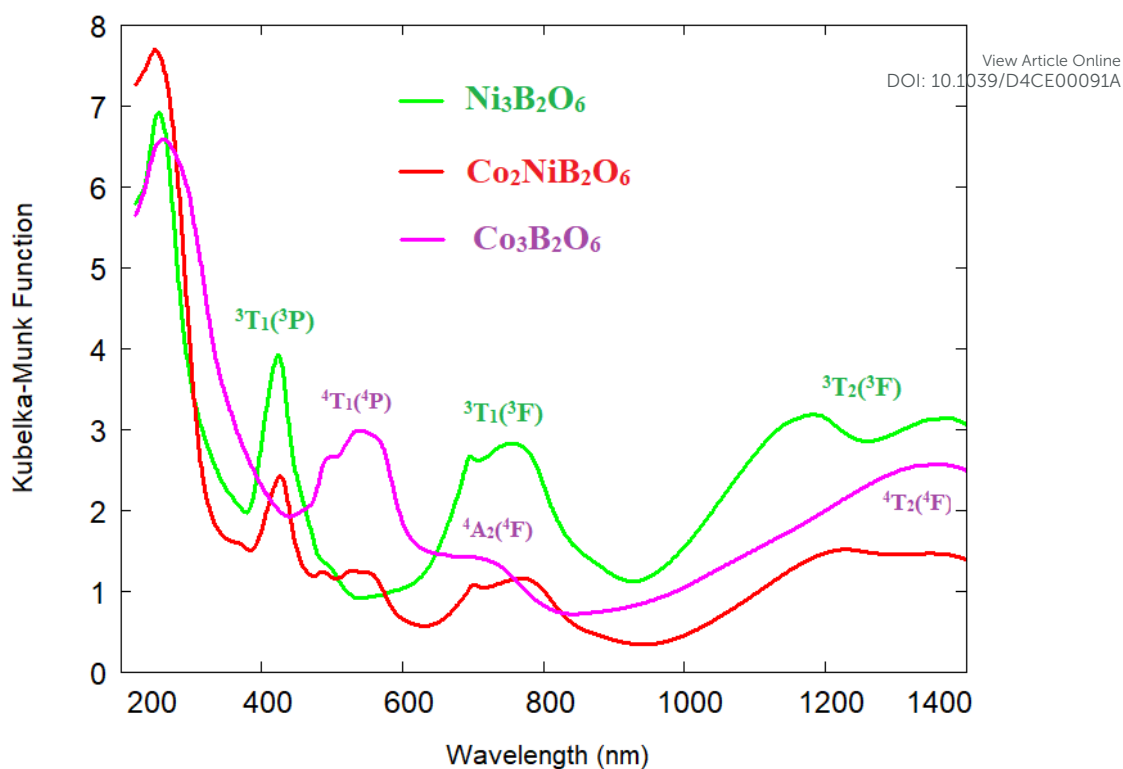


Fig. 5. The Kubelka-Munk functions of $\text{Ni}_3\text{B}_2\text{O}_6$, $\text{Co}_3\text{B}_2\text{O}_6$, and $\text{Co}_2\text{NiB}_2\text{O}_6$. The absorption bands upon the transitions from the ground state of Ni^{2+} ($^3\text{A}_2(^3\text{F})$) and Co^{2+} ($^4\text{T}_1(^4\text{F})$) ions to the corresponding excited states are denoted by green and purple, respectively.

The crystal field strength Dq and Racah parameter B can be obtained from the observed frequency values of two visible electronic transitions using the well-known technique described, e.g. in [23]. The values of Dq and B for Co^{2+} and Ni^{2+} in the kotoite structure appear to be rather close to each other: $Dq = 790.7 \text{ cm}^{-1}$ and $B = 864 \text{ cm}^{-1}$ for Co^{2+} and $Dq = 793 \text{ cm}^{-1}$ and $B = 866.6 \text{ cm}^{-1}$ for Ni^{2+} . The bands in the UV peaking at 254 nm for $\text{Ni}_3\text{B}_2\text{O}_6$, at 259 nm for $\text{Co}_3\text{B}_2\text{O}_6$ and at 250 nm for $\text{Co}_2\text{NiB}_2\text{O}_6$ can be assigned to charge transfer bands of the metal-to-ligand type. It should be noted that the obtained value of the Racah parameter for the nickel ion is close to the value obtained in [22] for the 4f position with the local symmetry C_2 , while it is significantly different from the Racah parameter for position 2a with the higher local symmetry C_{2h} . Thus, the results obtained can also support the assumption that in the $\text{Co}_2\text{NiB}_2\text{O}_6$ compound, nickel ions occupy position 4f.

Conclusions

We studied the conditions of crystal growth of solid solutions $\text{Ni}_{3-x}\text{Co}_x\text{B}_2\text{O}_6$ with the kotoite structure. From the flux system based on $\text{Bi}_2\text{Mo}_3\text{O}_{12}\text{-B}_2\text{O}_3$, which was diluted with carbonate Na_2CO_3 , we obtained four compositions of oxyborates with different content of transition metal ions. The composition of the compounds was determined using electron

scanning microscopy. The crystal structure of kotoite $\text{Co}_2\text{NiB}_2\text{O}_6$ was resolved using X-ray diffraction. The three compounds had the concentration of cobalt ions lower than 1. This would allow one to study the orientation of the easy axis in solid solutions of $\text{Ni}_{3-x}\text{Co}_x\text{B}_2\text{O}_6$, depending on the concentrations of cobalt ions. One can also trace how the lattice dynamics changes with the change in the concentration of cobalt ions. The distribution of magnetic cations over crystallographic positions is important for revealing magnetic properties. According to the theoretical calculations, nickel ions occupy the 4f crystallographic position, while cobalt ions occupy both crystallographic positions. The study of the diffuse scattering spectra and comparison of the Racah parameters for the compounds $\text{Ni}_3\text{B}_2\text{O}_6$ and $\text{Co}_2\text{NiB}_2\text{O}_6$ also indicate that nickel ions occupy crystallographic position 4f.

Thus, we obtained four compounds of the single crystal $\text{Ni}_{3-x}\text{Co}_x\text{B}_2\text{O}_6$ with different concentrations of cobalt ions. The composition and structural characteristics of all the compounds were determined. The theoretical and experimental studies show that nickel ions tend to occupy the 4f crystallographic position. Apart from the fundamental interest, the obtained crystals are a promising anode material for sodium-ion batteries.

Conflicts of interest

“There are no conflicts to declare.

Funding: The research was funded by Russian Science Foundation and Krasnoyarsk Regional Fund of Science, project № 23-12-20012 (<https://rscf.ru/en/project/23-12-20012/>).

Author contributions

Svetlana Sofronova – Conceptualization, Project administration, Supervision, Writing – original draft, Investigation; Evgeniya Moshkina – Investigation, Writing – original draft; Artem Chernyshev – Investigation; Aleksandr Vasiliev – Investigation; Nikolai G. Maximov – Investigation; Aleksandr Aleksandrovsky – Investigation, Writing – original draft; Tatyana Andryushchenko - Investigation; Aleksandr Shabanov – Investigation.

Acknowledgments: The experimental investigations were carried out in the Center for Collective Use of the Krasnoyarsk Regional Center of Research Equipment of Federal Research Center “Krasnoyarsk Science Center SB RAS”.

References

- [1] B. Xu, Yao Liu, Jianliya Tian, Xiao Ma, Qiushi Ping, Baofeng Wang иYongyao Xia, « $\text{Ni}_3(\text{BO}_3)_2$ as anode material with high capacity and excellent rate performance for sodium-ion batteries» *Chemical Engineering Journal* vol. 363 (2019) p. 285
- [2] Wang B et al, " A New Nickel/cobalt Borate as High-Performance Anode Material for Sodium-Ion, Batteries &Supercaps 2023, 6,.

[3] Karadas F et al. "Enhancing Oxygen Evolution Catalytic Performance of Nickel Borate with Cobalt Doping and Carbon Nanotubes", *Chemistry Select* 2023, 8, e202203561 (1 of 8)

[4] A. Debart, B. Revel, L. Dupont, L. Montagne, J.-B. Leriche, M. Touboul, and J.-M. Tarascon, Study of the Reactivity Mechanism of $M_3B_2O_6$ (with M - Co, Ni, and Cu) toward Lithium, *Chem. Mater.* (2003) vol. 15, pp. 3683-3691

[5] H. Yi, P. Xu, G. Shi, Z. Xiong, R. Wang, J. Shen, B. Wang, The manganese oxyborate $Mn_3(BO_3)_2$ as a high-performance anode for lithium-ion batteries, *Solid State Ionics* (2022) Vol. 380, p. 115935

[6] P. Liang, L. Du, X. Wang, Z.-H. Liu, Preparation of $Ni_3B_2O_6$ nanosheet-based flowerlike architecture by a precursor method and its electrochemical properties in lithium-ion battery, *Solid State Sciences* (2014) Vol. 37, pp. 131-135

[7] X. Sun, K. Zhao, Z. Liu, Z. Feng, Z. Wang, L. Cui, J. Liu, Facile electrodeposition of $Ni_3(BO_3)_2$ nanospheres on Ti mesh for high-performance asymmetric supercapacitors, *Journal of Energy Storage* (2022) vol. 55, Part D, p. 105763

[8] L. N. Bezmaternykh, S. N. Sofronova, N. V. Volkov, E. V. Eremin, O. A. Bayukov, I. I. Nazarenko and D. A. Velikanov Magnetic properties of $Ni_3B_2O_6$ and $Co_3B_2O_6$ single crystals, *Physica Status Solidi b* (2012) vol. 249, no. 8., pp. 1628-1633.

[9] R. V. Pisarev, M. A. Prosnikov, V. Y. Davydov, A. N. Smirnov, E. M. Roginskii, K. N. Boldyrev, A. D. Molchanova, M. Popova, M. B. Smirnov и V. Y. Kazimirov, Lattice dynamics and a magnetic-structural phase transition in the nickel orthoborate $Ni_3(BO_3)_2$, *Physical Review B* (2016) vol. 93, p. 134306.

[10] A. Molchanova, M. Prosnikov, V. Petrov, R. Dubrovin, S. Nefedov, D. Chernyshov, A. Smirnov, V. Davydov, K. Boldyrev, V. Chernyshev, R. Pisarev и M. Popova, Lattice dynamics of cobalt orthoborate $Co_3(BO_3)_2$ with kotoite structure, *Journal of Alloys and Compounds* (2021) vol. 865, p. 158797.

[11] B. Tekin and H. Güler, «Synthesis and crystal structure of dicobalt nickel orthoborate, $Co_2Ni(BO_3)_2$ » *Materials Chemistry and Physics* vol. 108(2008) pp. 88-91

[12] H. Güler and B. Tekin, «Synthesis and crystal structure $CoNi_2(BO_3)_2$ » *Inorganic Materials* vol. 45(2009) p. 538–542 [13] Moshkina E., Seryotkin Y., Bovina A., Molokeyev M., Eremin E., Belskaya N., Bezmaternykh L. Crystal formation of Cu-Mn-containing oxides and oxyborates in bismuth-boron fluxes diluted by MoO_3 and Na_2CO_3 // *J. Cryst. Growth.* – 2018. – V. 503. – P. 1–8.

[14] Moshkina E., Seryotkin Y., Bayukov O., Molokeyev M., Kokh D., Smorodina E., Krylov A., Bezmaternykh L. Flux Growth and Phase Diversity of Triple Oxides of Transition

Metals (Mn,Fe,Ga)₂O₃ in Multicomponent Fluxes Based on Bi₂O₃-MoO₃-B₂O₃-Na₂O // CrystEngComm. – 2023. – V. 25. – P. 2824-2834.

View Article Online
DOI: 10.1039/D4CE00091A

[15] Evgeniya Moshkina, Maxim Molokeev, Nadejda Belskaya, Ivan Nemtsev, Anastasiia Molchanova, Kirill Boldyrev, «Metastable growth and infrared spectra of CuB₂O₄:Ni single crystals» CrystEngComm, 23 (2021) pp. 6761-6768.
<https://doi.org/10.1039/D1CE00729G>

[16] Rousseau, R.V. The fundamental algorithm: a natural extension of the Sherman equation Part 1: Theory / R.M. Rousseau, J.A. Boivin // The Rigaku Journal. - 1998. - V. 15, No. 1. - p. 13-27

[17] F. Zhu, J. Liu, X. Lai, Y. Xiao, V. Prakapenka, W. Bi, E. Ercan Alp, P. Dera, B. Chen, J. L. Synthesis, «Elasticity, and Spin State of an Intermediate MgSiO₃-FeAlO₃ Bridgmanite: Implications for Iron in Earth's Lower Mantle» Journal of Geophysical Research: Solid Earth // - 2020 – V. 125 – P. e2020JB019964

[18] J. Kim; H. Kim; M. Chandran; S.-C. Lee; S. H. Im; K.-H. Hong «Impacts of cation ordering on bandgap dispersion of double perovskites» APL Mater. 6, 084903 (2018)

[19] E. K. Albrecht, A. J. Karttunen «Structural principles of cation ordering and octahedral tilting in A-site ordered double perovskites: ferroelectric CaMnTi₂O₆ as a model system» Dalton Trans. – 2022 – V. 51(43) – P. 16508-16516

[20] P. Blaha, K. Schwarz, G. Madsen, D. Kvasnicka and J. Luitz, «An Augmented Plane Wave + Local Orbitals Program for Calculating Crystal Properties», Vienna: Vienna University of Technology Inst. of Physical and Theoretical Chemistry, 2015.

[21] P. Blaha, K. Schwarz, F. Tran, R. Laskowski, G. Madsen и L. Marks, «WIEN2k: An APW+lo program for calculating the properties of solids» J. Chem. Phys. vol. 152 (2020) p. 074101.

[22] J. Perdew and Y. Wang, «Accurate and simple analytic representation of the electron-gas correlation energy» Physical Review B vol. 45 (1992) p. 13244.

[23] J. P. Perdew, K. Burke and M. Ernzerhof, «Generalized Gradient Approximation Made Simple» Physical Review Letters vol. 77 (1996) p. 3865.

[24] V. I. Anisimov, J. Zaanen and O. K. Andersen, «Band theory and Mott insulators: Hubbard U instead of Stoner I» Physical Review B vol. 44(1991) p. 943.

[25] V. I. Anisimov, I. V. Solovyev, M. A. Korotin, M. T. Czyżyk and G. A. Sawatzky, «Density-functional theory and NiO photoemission spectra» // Physical Review B vol. 48 (1993) p. 16929.

[26] Gurusamy Sivakumar and Srinivasan Natarajan, «Structural evolution of transition metal orthoborates ($Zn_3B_2O_6$ - $Co_3B_2O_6$) with the Kotoite mineral structure: Synthesis, structure and properties» *Z. Anorg. Allg. Chem.* 648 (2022)e202200017

[View Article Online](#)

[DOI: 10.1039/C4CE00001A](#)

[27] A. D. Molchanova «Experimental Study and Analysis of Absorption Spectra of Ni^{2+} Ions in Nickel Orthoborate $Ni_3(BO_3)_2$ » *Physics of the Solid State*, vol. 60 (2018) pp. 1957–1965

[28] A. E. Underhill and D.E. Billing, «Calculations of the Racah Parameter B for Nickel (II) and Cobalt (II) Compounds» *Nature*, Vol. 210 (1966) p. 834